Received: 15 July 2020 | Revised: 22 October 2020 | Accepted: 23 November 2020

DOI: 10.1002/ddr.21768

RESEARCH ARTICLE

DRUG DEVELOPMENT RESEARCH WILEY

Design of multicomponent indomethacin-paracetamol and famotidine loaded nanoparticles for sustained and effective anti-inflammatory therapy

Mohyeddin Assali | Nihal Zohud

Department of Pharmacy, Faculty of Medicine and Health Sciences, An-Najah National University, Nablus, Palestine

Correspondence
Mohyeddin Assali, Department of Pharmacy, Faculty of Medicine and Health Sciences, An-Najah National University, Nablus, Palestine.
Email: m.d.assali@najah.edu

Abstract

Indomethacin is one of the nonsteroidal anti-inflammatory drugs (NSAIDs) that are widely prescribed drug for pain and inflammation. However, its notoriety of causing gastrointestinal effect, low water solubility, and its short half-life would affect patient compliance and its oral absorption and accordingly justify the need to develop a formula with a controlled and sustained release manner in combination with anti-ulcer drugs. Herein, we synthesized indomethacin-paracetamol co-drug loaded in nanoemulsion and encapsulated in famotiditine loaded polycaprolactone (PCL) nanoparticles. The synthesis of the co-drug was achieved by the formation of a hydrolyzable ester between the indomethacin and paracetamol. The synthesized co-drug was preloading in nanoemulsion (Co-NE), which encapsulated into famotidine PCL nanoparticles utilizing the nanoprecipitation approach. The developed nanosystem showed hydrodynamic size less than 200 nm and the zeta potential value above −30 mV. TEM images confirmed the morphological structure of the formed nanoemulsion and the loaded PCL nanoparticles. Stability studies revealed that the developed nanosystem was stable at different temperatures and pHs over 1 month. Moreover, improvement of the solubilities of these three drugs leading to have a controlled-release multicomponent system of both co-drug and famotidine over 3 days. This multicomponent nanoparticle might be a potential platform to overcome the obstacles of NSAIDs, synergize drugs with different mechanisms of actions by co-encapsulating a small-sized nanoemulsion into PCL nanoparticles for reaching the goal of effective anti-inflammatory therapy.

KEYWORDS

D-limonene, esterase, kinetic release study, nanoemulsion, polycaprolactone nanoparticles, sustained release

1 | INTRODUCTION

Inflammation is a nonspecific, natural, and cellular response to multiple stimuli like infection, injury, irritation, and microorganisms promoting the release of different protective chemicals (Laroux, 2004). Among these chemicals are prostaglandins (PGs) which are hormone-like mediators that play a crucial role in the inflammatory processes (Ricciotti & FitzGerald, 2011). Inflammation is an essential status leading to the elimination of insulting factors and rejuvenation of tissue structure and physiological function (Nathan, 2002). Nonsteroidal anti-inflammatory drugs (NSAIDs) are among the most commonly prescribed and consumed drugs for pain and inflammation worldwide (Badri et al., 2016; Hochberg et al., 2012). They act by blocking the prostaglandin synthesis through the inhibition of cyclooxygenase

(COX) enzymes which is responsible for the desired anti-inflammatory activity and the unwanted gastrointestinal effects (Higuchi et al., 2009; Sostres et al., 2010). For various chronic diseases such as rheumatoid arthritis, osteoarthritis, and ankylosing spondylitis, NSAIDs are often prescribed using high doses which often cause many side-effects and poor patient compliance. Therefore, those drugs require strict monitoring, especially in patients with renal and cardiovascular diseases (Amadio Jr et al., 1997).

Indomethacin (IND) is considered one of the most potent non-selective NSAIDs owning very effective antipyretic, analgesic, and anti-inflammatory activities (Yeh, 1985). It is chemically classified as a derivative of indoleacetic acid (Fritsche et al., 2001) with low water solubility and a short half-life of 4–5 h, causing multiple daily doses prescription (Clarysse et al., 2009; Ziltener et al., 2010). It is most typically used for the treatment of inflammation resulting from rheumatoid diseases. The nonselective inhibitory activity of COX enzymes and the undesirable physical property (poor solubility) are responsible for the gastrointestinal (GI) irritation side effects (Alsaidan et al., 1998; Saeedi et al., 2011). Furthermore, it can cause CNS disruption especially a frequent headache (Lucas, 2016). Therefore, various studies were reported to reduce the mentioned side effects through indomethacin encapsulation or conjugation in proper nano-vehicles (Giacomelli et al., 2007; Tan et al., 2018).

Several studies showed combining NSAIDs with paracetamol (PAR) results in synergistic analgesia and decreases the required dose which would reduce the raised adverse effects (Ong et al., 2010). Furthermore, famotidine (FAM) is widely used for the treatment of acid-related GI conditions, and it was found to be effective in preventing gastric injury caused by Indomethacin, even at the lowest dose (Naito et al., 2008). FAM is a competitive inhibitor of histamine H_2-receptor that blocks histamine actions by binding to the histaminic receptor located on the parietal cells of the stomach resulting in inhibition of gastric secretion (Berlin et al., 1986; Talke & Solanki, 1993). FAM improves ulcer healing and reverses the GI side effects of IND by inhibiting the secretion of gastric acid and also by increasing collagen secretions (Hassan et al., 1997; Perez-Aisa et al., 2003).

On this point, combination therapy through combining multiple treatments with various mechanisms is a highly effective strategy in the treatment of various diseases like cancer, inflammatory diseases, HIV, and others (Baek et al., 2017; Baek & Cho, 2015; Coradini et al., 2015; Freeling et al., 2014). To achieve this approach, different drug delivery systems based on suitable nanomaterials and capable of behaving combinations of various therapies have been successfully explored (Gadde, 2015). Therefore, we designed multidrug delivery systems that allow the sustained release of IND-PAR co-drug and FAM encapsulated in polycaprolactone (PCL) nanoparticles.

Herein, a co-drug of indomethacin and paracetamol (IND-PAR) was synthesized and encapsulated in fruit flavor nanoemulsion (NE) containing limonene as it masks the unpleasant bitter taste and promotes gastric ulcer healing by increasing mucus production and enhances the solubility and bioavailability of the co-drug (de Souza et al., 2019; Gursoy & Benita, 2004; Mohsin et al., 2009; Moraes et al., 2013). The co-drug loaded nanoemulsion was then encapsulated into PCL nanoparticles containing FAM using nanoprecipitation technique as shown in Scheme 1. We chose PCL as it is considered a biodegradable polymer with exceptional rheological and viscoelastic properties, high drug permeability, and long stability (Guarino et al., 2017; Nair & Laurencin, 2007; Woodruff & Hutmacher, 2010). The in vitro release profiles of co-drug and FAM in the developed multidrug nano delivery system were investigated in addition to stability and biocompatibility studies on cells were executed.

2 | MATERIALS AND METHODS

2.1 | Reagents and materials

PCL, D-limonene were purchased from Sigma-Aldrich Company. Polyoxyethylene cetyl ether (POE) and polyvinyl alcohol (PVA) were purchased from CS Company, New Zealand. Sorbitan monooleate (Span® 80) was purchased from Alfa Aesar, UK. Polyoxyethylene sorbitan monooleate (Tween® 80) was purchased from Arcos organics. Acetone, methanol (MeOH), dichloromethane (DCM), and isopropyl alcohol were purchased from C.S. Company, Haifa. Disodium hydrogen phosphate, potassium hydrogen phosphate, sodium carbonate, and sodium bicarbonate were purchased from CS company, Haifa. Spectra/Por® four dialysis membranes (12–14 KD MWCO, 25 mm flat width, 100 ft length) were purchased from Spectrum Laboratories, Inc. Porcine liver esterase (PLE) was purchased from Sigma-Aldrich. Dulbecco's free Ca^{+2} phosphate-buffered saline and L-glutamine solution, Pen-Strep Solution were purchased from Biological Industries, Jerusalem. RPMI was purchased from Manassas VA, Trypsin–EDTA solution 1X, fetal Bovin Serum, trypan blue solution, and MTS kit were purchased from Promega.

2.2 | Techniques and instruments

Dynamic light scattering (DLS) and zeta potential analysis were measured on NanoBrook Omni (Brookhaven Instruments). High-performance liquid chromatography with binary HPLC pump and

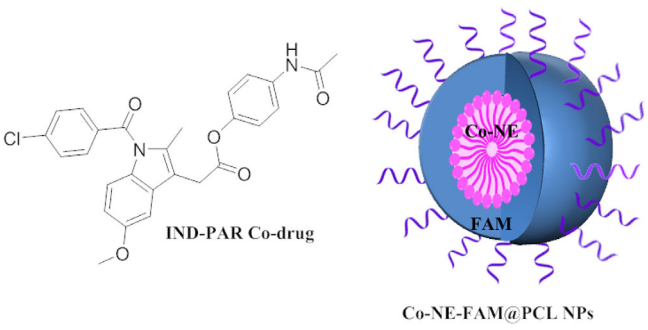

SCHEME 1 The general scheme demonstrates the chemical structure of the co-drug and the general approach of the study

waters 2298 photodiode Array Detector (Waters 1525) were utilized to quantify drugs. Transition electron microscope (TEM) images were taken at 60 kV using Morgagni 286 transmission microscope (FEI Company, Eindhoven, Netherlands). Esco cell culture CO_2 incubator was used to incubate the cell line. Unilab microplate reader 6000 was utilized in the cell viability test to read the plate.

2.3 | Synthesis of IND-PAR co-drug

The synthesis and characterization of IND-PAR co-drug have been developed and published recently (Assali et al., 2020).

2.4 | Preparation of nanoemulsion

The method of nanoemulsion preparation was developed using the ultrasonication method (Li & Chiang, 2012a). In brief, the organic phase consists of 140 mg of sorbitan monolaurate (Span® 80) and 750 mg of D-limonene which was sonicated for 5 min. After that, it was added dropwise under mild stirring to the aqueous phase that consists of 360 mg of tween 80 and 8.75 ml of milli-Q water. The resultant flocculated emulsion was mildly stirred for 15 min and sonicated for 10 min to obtain a blank nanoemulsion. To load the co-drug in the nanoemulsion, 2 mg of the co-drug was added into the organic phase and following the same mentioned procedure to obtain co-drug encapsulated in nanoemulsion (Co-NE). Finally, the hydrodynamic size, polydispersity index (PDI), and zeta potential were measured. The measurements were taken at 25°C and using 90° of the angle scattering. The ζ-potential measured using the phase analysis light scattering (PALS) technique.

2.5 | Preparation of polymeric nanoparticles

Nanoprecipitation technique was used for the preparation of PCL nanoparticles (Assali, Shawahna, Shareef, & Alhimony, 2018b; Assali, Zaid, Bani-Odeh, et al., 2017). Briefly, the organic component consists of 25 mg of PCL and 5 mg POE dissolved in 5 ml acetone which was added drop-wisely to the aqueous component consisting of 3 g of 1% PVA and 7 ml of Milli-Q water under mild stirring. The resulting suspension was stirred mildly for 30 min and then, the solvent (acetone) evaporated by rotary evaporator. After that, a 0.45 μm pore size membrane syringe filter was used to filtrate the solution to get a uniform particle size. Purification of the formed nanoparticles was performed by centrifugation at 15000 rpm for 10 min and washed three times with Milli-Q water to remove any residual of PVA. The obtained nanoparticles were dissolved in 2 ml milli-Q water and stored in a refrigerator. Finally, effective diameter, PDI, and zeta potential were determined using DLS.

To prepare PCL nanoparticles loaded with the Co-NE and FAM, 1 ml of the well-characterized Co-NE and 2 mg FAM were added to the aqueous phase and following the same procedure as mentioned above.

HPLC analytical method was developed and validated to measure the loaded amount of drugs according to our recently published method (Assali et al., 2020).

After that, the percentage of the encapsulation efficiency (EE) for FAM and co-drug was calculated using the following equation.

$$\mathbf{EE}\,(\%) = (\text{weight of drug} - \text{loaded in the nanoparticles})/(\text{weight of drug initially used}) \times 100\%.$$

2.6 | In vitro release studies

2.6.1 | In vitro release of co-drug and FAM from PCL NPs without esterase enzyme

Ten milligram of freeze-dried samples Co-NE-FAM@PCL nanoparticles were dissolved in 3 ml freshly prepared phosphate buffer saline (PBS) at pH 7.4 and then transferred into a dialysis bag (donor compartment). This bag was firmly closed, then was placed into 40 ml of PBS at pH 7.4 (receptor compartment), fully immersed, and gently stirred for more than 3 days at 37°C. Aliquots of 1 ml from each receptor compartment were taken and replaced directly with 1 ml freshly prepared PBS pH 7.4 at determined periods. These samples were analyzed using HPLC and percentage release of co-drug and FAM were calculated along the time.

2.6.2 | In vitro hydrolysis of co-drug loaded in nanoemulsion and PCL nanoparticles

The synthesized co-drug was exposed to esterase enzyme to study its hydrolysis to its parent drugs (IND & PAR). One milligram of co-drug was incubated in 10 ml PBS containing 2 mg of esterase enzyme at 37°C for 1 h (Assali et al., 2016; Assali et al., 2019; Assali, Zaid, Abdallah, et al., 2017). For the in vitro hydrolysis of co-drug in NE or PCL nanoparticles, the same procedure was followed by adding 1 ml of Co-NE or Co-NE-FAM@PCL nanoparticles into the same aforementioned media and gently stirred for 5 h. At different time intervals, aliquots of 1 ml were obtained and replaced with equal volumes of fresh BPS to mimic the sink conditions, filtered using a 45 μm syringe filter, and then analyzed by HPLC. Percentage hydrolysis and percentage conversion of co-drug were determined using the developed HPLC validated method.

2.7 | Drug release kinetics

To assess the release mechanism of both co-drug and FAM from the designed and formulated nanosystems, different kinetic models were applied using the DDsolver program which helps to get satisfied dissolution data modeling and analysis. A comparison between each model and each nanosystem was based on the linear regression

($R^2_{adjusted}$) (P. Costa & Lobo, 2001), the akaike information criterion (AIC) (Akaike, 1974b), and the model selection criterion (MSC). Data analysis was performed using the Excel add-in DDSolver program and the best-fitted models were taken based on the higher $R^2_{adjusted}$ and the lower AIC and MSC values more than 2.0.

2.8 | Stability studies at different temperatures and pH buffers

2.8.1 | Stability studies at different temperature

The stability of Co-NE-FAM@PCL nanoparticles was tested at different temperatures (4–8, 25, and 40°C). One milliliter of nanoparticles was stored at the required temperature and aliquots were taken at specified time intervals for ~1 month. Each aliquot was tested by DLS, polydispersity, and zeta potential analysis.

2.8.2 | Stability studies using different buffers

The stability of Co-NE-FAM@PCL nanoparticles was determined at two different buffers (acetate pH = 4.2 and carbonate pH = 9.4) by diluting 1.5 ml of nanoparticles with 1.5 ml of each buffer, and aliquots were taken for DLS and zeta potential measurements during 1 month.

2.9 | Cell biocompatibility tests

2.9.1 | Cell line

The cytotoxicity of the Co-NE-FAM@PCL nanoparticles was investigated on HeLa cells and 3 T3 fibroblasts.

2.9.2 | Cell culture

The cells were cultured in T-175 cell culture flasks supplemented with cell culture growth medium (CGM) composed of RPMI basal medium supplemented with L-glutamine (1%), FBS (10%), and penicillin/streptomycin (1%). The cells were kept in a standard cell culture incubator at 5% CO_2, 37°C, and 99% humidity.

For sub-culturing, the medium was suctioned and washed with an excess of Ca^{2+}-free PBS. After that, the cells were incubated with 0.025% trypsin for up to 5 min in the cell culture incubator until sufficient cells detached from the flask. Then trypsin was inactivated by CGM, the cell suspension was collected and the viable cell count was determined using trypan blue stain before adjusting the cell concentration to 50.000 cell/ml. Finally, the cells were seeded in a 96-well plate as 5000 cells/well. The cells were left to adhere and accommodate overnight before running any test.

2.9.3 | Cell biocompatibility test

HeLa cells and 3 T3 fibroblasts were seeded in 96-well plates and then incubated with 100 µl per well CGM supplemented with different concentrations of the tested Co-NE-FAM@PCL nanoparticles for 24 h. After that, they were incubated for 2 h at 37°C and 5% CO_2 with 20 µl per well of MTS reagent. Lastly, the absorbance of each concentration was determined by a plate reader at a wavelength of 490 nm. The percentage of viability was calculated by the following equation:

$$\%\text{viability} = (\text{abs of treated cells} - \text{abs of blank}) / (\text{abs of control cells} - \text{abs of blank}) \times 100\%$$

3 | RESULTS AND DISCUSSION

3.1 | Synthesis of the co-drug and preparation of PCL nanoparticles

Indomethacin is one of the potent anti-inflammatory drugs that inhibit COX enzymes but induces gastric ulcer and has a short half-life. Herein, we developed a new multicomponent nano-drug delivery system composed of IND-PAR co-drug nanoemulsion encapsulated in FAM PCL nanoparticles to reduce the required dose, side effects, and provide a sustained release profile to improve patient compliance. In this regard, we have recently synthesized a co-drug of IND-PAR connected through a well-known hydrolyzable ester bond that can easily be converted to the parent drugs in the presence of esterase enzyme as shown in Scheme 2 (Assali et al., 2020).

The synthesized IND-PAR co-drug was then encapsulated in a small-sized D-limonene flavored nanoemulsion (NE) to improve the water solubility of the co-drug and provide a pleasant flavor to the formula. The nanoemulsion was composed of two nonionic and biocompatible surfactants TWEEN 80 and SPAN 80 that can mix easily and form a stable o/w nanoemulsion (Koroleva et al., 2018). Moreover, various studies showed the addition of D-limonene provides higher stability, better taste, odor, and decreases the particle size of the formed o/w nanoemulsion (Li & Chiang, 2012a). Interestingly, D-limonene promotes gastric ulcer healing by increasing mucus production and displays anti-inflammatory activity (de Souza et al., 2019; Moraes et al., 2013).

The resulting yellowish o/w nanoemulsion was characterized by TEM to study the size and the morphology of the formed nanoemulsion. Figure 1 showed the formation of the spherical shape of the nanoemulsion with a size of ~2 nm in diameter. The formed transparent solution of the micelle structure represents ultra-small micelles formation that is dispersed in the aqueous phase. The very small size of the formed micelle is due to the addition of the oil-soluble D-limonene that could easily homogenize the formed aggregates of the surfactants and facilitate the diffusion of the surfactant in the

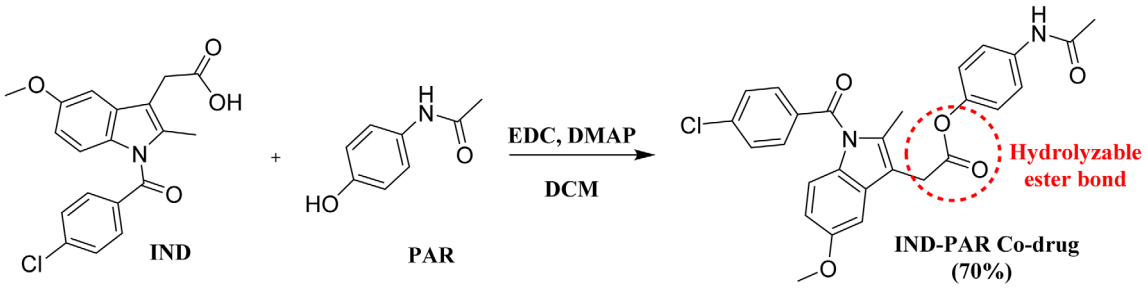

SCHEME 2 Synthetic scheme of indomethacin-paracetamol co-drug

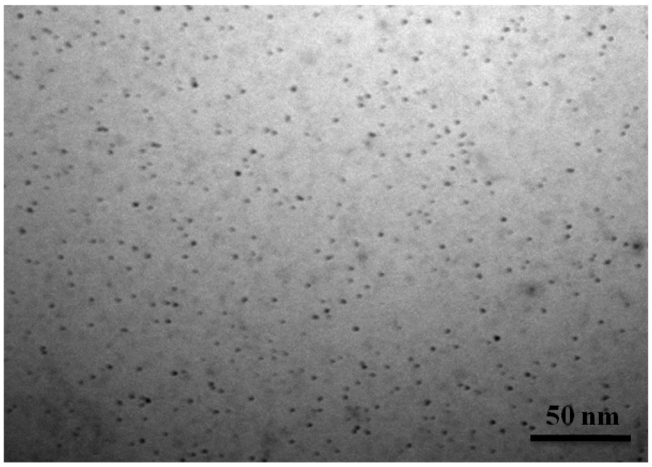

FIGURE 1 TEM image showed the morphology of the formed nanoemulsion

aqueous phase (Aziz et al., 2019; Chang et al., 2013; Chang & McClements, 2014; Kuznetsova et al., 2020). Moreover, the utilization of the ultrasonication has additional assistance to ease the formation of ultrasmall micellar structure (Li & Chiang, 2012). Moreover, the formed nanoemulsion was further characterized by DLS and zeta potential analyzer to determine the hydrodynamic diameter size, polydispersity index (PDI), and zeta potential as shown in Table 1. The small particle size of the formed NE was obtained in the range of 1.5–2.5 nm. Zeta potential values demonstrate the net charge on the surface of nanomaterials; enhance their physical state in liquids and accordingly their interactions with biological systems. Zeta potential values were higher than ±25 mV considered highly stable nanomaterials (Bhattacharjee, 2016). In our case, we obtained nanoemulsions with zeta potential values were above −35 mV which indicates the formation of high stable nanoemulsions. It was noticed that the size was slightly increased in the co-drug loaded nanoemulsion as a consequence of co-drug loading with a loading capacity of 100%. Therefore, we formed a small-sized, monodisperse, stable, and monodisperse fruit-flavor Co-NE which allowed for greater absorption due to small-sized droplets with greater surface area (Jaiswal et al., 2015).

TABLE 1 Characterization of blank and co-NEs

	Blank NE (blank)	Co-NE
Hydrodynamic size (nm)	1.64	2.33
Polydispersity index	0.162	0.272
Zeta potential (mV)	−38.02	−47.77

Once the Co-NE was successfully prepared and characterized, it was encapsulated into PCL nanoparticles using the nanoprecipitation method developed previously in our research group (Assali, Shawahna, Dayyeh, Shareef, & Alhimony, 2018a; Assali, Zaid, Bani-Odeh, et al., 2017). The developed nanoparticles were decorated with polyethylene oxide which acts as a masking agent against opsonization for the drug transporter and accordingly prevents phagocytosis by mononuclear phagocyte system (MPS) (Torchilin & Trubetskoy, 1995). Upon the preparation of the PCL nanoparticles, the Co-NE and FAM were added to the organic layer to form Co-NE-FAM@PCL nanoparticles. The prepared nanoparticles were characterized by TEM, DLS, and zeta potential analysis as shown in Figure 2, and Table 2. Figure 2 shows the TEM image of blank PCL nanoparticles obtaining large and rounded nanoparticles with a diameter range between 150 and 200 nm. However, Figure 2b shows the TEM image of Co-NE-FAM@PCL nanoparticles demonstrating the formation of spherical nanoparticles with a double layer of nanoemulsion surrounded by the PCL nanoparticles and a diameter size in the range of 170–210 nm.

Table 2 shows the hydrodynamic diameters, PDI, and zeta potential data for the blank and loaded PCL nanoparticles. The values showed the formation of nanoparticles with a hydrodynamic diameter between 170 and 200 nm, monodisperse nanoparticles as the values of PDI less than 0.3, and high stable solutions with zeta potential values above −25 mV.

In order to determine the loading capacity of co-drug and FAM, and the in vitro release profiles, a validated HPLC method was developed and recently published (Assali et al., 2020). From the developed calibration curves and applying the encapsulation efficiency (EE) equation, we obtained high values EE of 100% and 85% for co-drug and FAM, respectively, which demonstrated the effectiveness of PCL in encapsulating Co-NE and FAM.

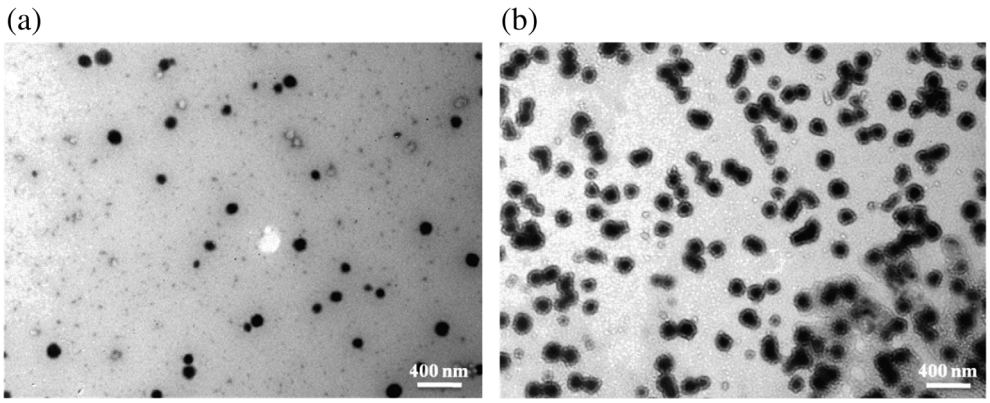

FIGURE 2 TEM image of (a) Blank PCL nanoparticles; (b) Co-NE-FAM@PCL nanoparticles

TABLE 2 Characterization of PLGA and PCL nanosystems

	Blank PCL NPs	Co-NE-FAM@PCL NPs
Hydrodynamic size (nm)	171.0	196.4
PDI	0.074	0.216
Zeta potential (mV)	−27.19	−39.42

3.2 | In vitro release studies

The developed HPLC analytical method was utilized to investigate the in vitro conversion of co-drug to its parents' drugs (IND-PAR) at nano-emulsion (Co-NE), and co-drug in PCL nanoparticles (Co-NE-FAM@PCL) in the presence of esterase enzyme (1 U/ml) in PBS (pH 7.4) 37°C.

3.2.1 | Percentage of conversion at Co-NE and Co-NE-FAM@PCL

For the conversion of the co-drug to IND-PAR, we used esterase enzyme through the incubation with PLE enzyme, a decrease in the co-drug HPLC peak with a concomitant increase of IND-PAR HPLC peaks, and this conversion was quantified by the developed equations. As seen in Figure 3, more than 80% of the co-drug was converted to IND and PAR after almost 6 h of incubation which confirms the successful conversion and hydrolysis of ester bond to the active pharmacological drugs.

3.2.2 | In vitro release of co-drug and FAM without PLE

The in vitro release profiles of co-drug and FAM were investigated using the dialysis membrane technique. It observed an initial burst of about 22% of co-drug from the PCL nanoparticles especially in the first 20 min followed by a sustained release of about 90% for co-drug for more than 3 days as displayed in Figure 4 red line. However, the release profile of FAM was about 40% after 20 min and followed by a rapid increase of about 80% with a sustained release for more than 80 h, as can be observed in Figure 4 black line. Therefore, FAM was firstly released from the shell of the PCL nanoparticles to provide a gastro-protective effect followed the sustained release manner of the co-drug from the nano-emulsion core of the PCL nanoparticles as can be observed in Figure 4.

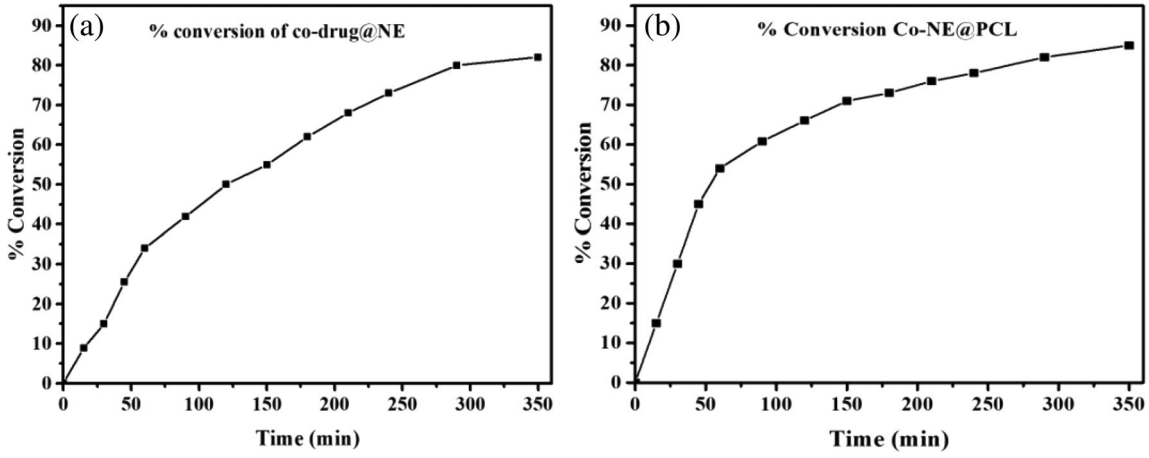

FIGURE 3 (a) % conversion of co-drug loaded in the nanoemulsion; (b) % conversion of co-drug loaded co-NE-FAM@PCL nanoparticles

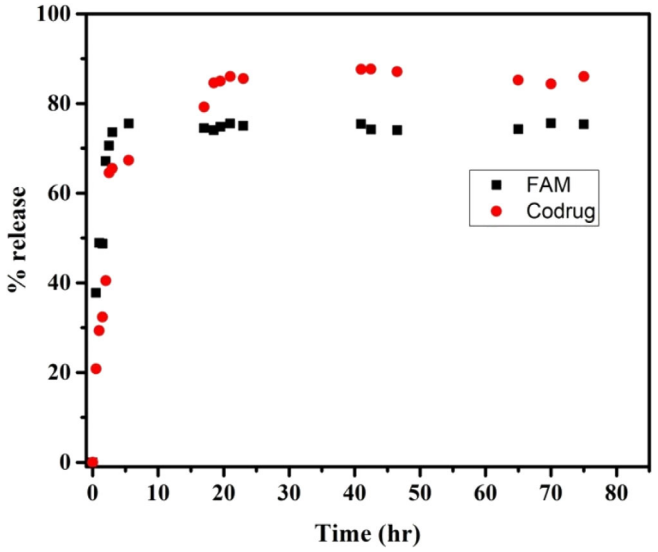

FIGURE 4 % release of co-drug and FAM from co-NE-FAM@PCL nanoparticles

TABLE 3 The most fitted models for both nanosystems

Drug	Kinetic model	$R^2_{adjusted}$	AIC	MSC
FAM	Weibull	0.9756	100.79	2.51
Co-drug	First-order with Fmax	0.9705	116.98	2.98

3.3 | Drug release kinetics

The kinetic models of the in vitro release were investigated. To discriminate the most appropriate model, $R^2_{adjusted}$, the AIC, and the MSC were determined (Akaike, 1974a; Handbook, 1995). The best kinetic model should show the highest coefficient of determination $R^2_{adjusted}$ (Costa & Lobo, 2001), the lowest Akaike Information (AIC) (F. Costa et al., 2003), and a value of more than two of MSC (Koizumi et al., 2001; Mayer et al., 1999).

The results for the curve-fitting studies revealed that FAM release from PCL nanoparticles could be best described by the Weibull model whereas first-order with F_{max} would be the best for co-drug as seen below in Table 3. As can be observed, the R^2 for FAM and co-drug was above 0.97, AIC values were the lowest, and MSC values were above two for both drugs as represented in Table 3. It was noted the best model of the FAM Weibull model which suggested that FAM was released from the spherical polymeric matrix with a sustained release manner. Interestingly, Weibull which is known as stretched exponential is the most common model applied to fit diffusion-controlled experimental data (Ignacio et al., 2017; Kosmidis et al., 2003).

The most suitable model for co-drug was first order with maximum release fraction (F_{max}) value 85.99% of co-drug, where the rate was concentration-dependent and this result was in accordant with co-drug hydrolysis in which first-order kinetic model was the most suitable.

3.4 | Stability studies

The stability of Co-NE-FAM@PCL nanoparticles was investigated by varying the temperatures (4–8, 25, and 40°C) and the pH (4.2 and 9.4). It was studied by analyzing the size of particles and the zeta potential as a function of time. It was obvious from Table 4 that the nanoparticles were stable at the three different temperatures and the two buffer conditions as particle size and polydispersity changes are within the acceptable limits and do not exceed a size above 220 nm and polydispersity also less than 0.3 for all measurements and that results were with the agreement that PCL polymer considered as a long-term stable polymer (Woodruff & Hutmacher, 2010). Moreover, zeta potential measurements were taken for the last readings and confirm high stability for the whole period of the study (1 month) where the values were above −30 mV.

3.5 | Cellular biocompatibility

It is very essential to determine the biocompatibility of the developed nanoparticles. For that reason, we have investigated the cellular compatibility on HeLa cells and 3 T3 fibroblast cells. The viability test was performed using MTS assay to determine the percentage of viability of the cells upon their incubation with the developed nanosystem after 24 h. As can be observed in Figure 5, both cell lines were incubated with various concentrations (25–400 μg/ml) of the developed nanosystem. The results showed excellent viability of both cell lines in comparison to the control without any statistical difference in any tested concentration which confirms the biocompatibility of the developed Co-NE-FAM@PCL nanoparticles.

TABLE 4 Stability study of co-NE-FAM@PCL NPs at different temperatures and buffers

	Temperature (°C)			Buffers	
	4–8	*25*	*50*	*Acetate*	*Carbonate*
Hydrodynamic size (nm) on the first day.	189.29	178.03	222.13	209.38	214.77
Polydispersity index on the first day.	0.190	0.176	0.134	0.100	0.128
Hydrodynamic size (nm) after 1 month.	229.60	181.19	214.71	206.33	206.07
Polydispersity after 1 month.	0.061	0.196	0.181	0.152	0.187
Zeta potential after 1 month.	−30.48	−32.31	−33.53	−45.22	−42.61

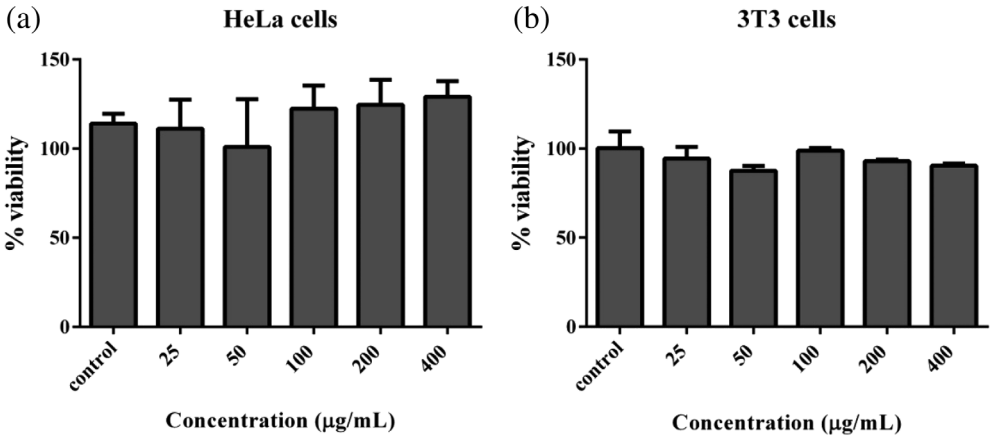

FIGURE 5 Viability assay of co-NE-FAM@PCL nanoparticles incubated with (a) HeLa cells; (b) 3 T3 fibroblast

4 | CONCLUSION

In this study, a multicomponent nanosystem was successfully designed and obtained for effective anti-inflammatory therapy based on nanoemulsion and PCL nanoparticles. This nanosystem was achieved by loading the synthesized IND-PAR co-drug into a fruit-flavor nanoemulsion followed by the encapsulation of the latter into PCL nanoparticles containing FAM in its core. These nanosystems were characterized using different techniques and their sustained release manners and hydrolysis of co-drug were studied by a novel, developed, and validated RP-HPLC analytical method. The developed nanosystem showed high biocompatibility and had good stability at different conditions. Subsequently, it is a promising platform for overcoming the obstacles of NSAIDs and enhancing patient compliance with their therapy.

ACKNOWLEDGMENT

Nihal Zohud acknowledges the Faculty of Graduate Studies at An-Najah National University to facilitate the achievement of this work. The authors thank Duaa Qattan at the University of Jordan for her assistance in the TEM analysis.

CONFLICT OF INTEREST

Authors declare no conflict of interest.

DATA AVAILABILITY STATEMENT

The data used to support the findings of this study are included within the article.

ORCID

Mohyeddin Assali https://orcid.org/0000-0002-2286-9343

REFERENCES

Akaike, H. (1974). A new look at the statistical model identification. *IEEE Transactions on Automatic Control*, *19*(6), 716–723.

Alsaidan, S. M., Alsughayer, A. A., & Eshra, A. G. (1998). Improved dissolution rate of indomethacin by adsorbents. *Drug Development and Industrial Pharmacy*, *24*(4), 389–394.

Amadio, P., Jr., Cummings, D. M., & Amadio, P. B. (1997). NSAIDs revisited: Selection, monitoring, and safe use. *Postgraduate Medicine*, *101*(2), 257–271.

Assali, M., Abualhasan, M., Zohud, N., & Ghazal, N. (2020). RP-HPLC method development and validation of synthesized Codrug in combination with indomethacin, Paracetamol, and famotidine. *International Journal of Analytical Chemistry*, *2020*, 1–9. https://doi.org/10.1155/2020/1894907.

Assali, M., Joulani, M., Awwad, R., Assad, M., Almasri, M., Kittana, N., & Zaid, A. N. (2016). Facile synthesis of ciprofloxacin Prodrug analogues to improve its water solubility and antibacterial activity. *Chemistry Select*, *1*(6), 1132–1135. https://doi.org/10.1002/slct.201600091.

Assali, M., Kittana, N., Qasem, S. A., Adas, R., Saleh, D., Arar, A., & Zohud, O. (2019). Combretastatin A4-camptothecin micelles as combination therapy for effective anticancer activity. *RSC Advances*, *9*(2), 1055–1061. https://doi.org/10.1039/c8ra08794f.

Assali, M., Shawahna, R., Dayyeh, S., Shareef, M., & Alhimony, I.-A. (2018). Dexamethasone-diclofenac loaded polylactide nanoparticles: Preparation, release and anti-inflammatory activity. *European Journal of Pharmaceutical Sciences*, *122*, 179–184. https://doi.org/10.1016/j.ejps.2018.07.012.

Assali, M., Zaid, A. N., Abdallah, F., Almasri, M., & Khayyat, R. (2017). Single-walled carbon nanotubes-ciprofloxacin nanoantibiotic: Strategy to improve ciprofloxacin antibacterial activity. *International Journal of Nanomedicine*, *12*, 6647–6659. https://doi.org/10.2147/ijn.s140625.

Assali, M., Zaid, A. N., Bani-Odeh, M., Faroun, M., Muzaffar, R., & Sawalha, H. (2017). Preparation and characterization of carvedilol-loaded poly (d, l) lactide nanoparticles/microparticles as a sustained-release system. *International Journal of Polymeric Materials and Polymeric Biomaterials*, *66*(14), 717–725.

Aziz, Z. A. A., Nasir, H. M., Ahmad, A., Setapar, S. H. M., Ahmad, H., Noor, M. H. M., Rafatullah, M., Khatoon, A., Kausar, M. A., Ahmad, I., Khan, S., al-Shaeri, M., & Ashraf, G. M. (2019). Enrichment of eucalyptus oil nanoemulsion by micellar nanotechnology: Transdermal analgesic activity using hot plate test in rats' assay. *Scientific Reports*, *9*(1), 13678. https://doi.org/10.1038/s41598-019-50134-y.

Badri, W., Miladi, K., Nazari, Q. A., Greige-Gerges, H., Fessi, H., & Elaissari, A. (2016). Encapsulation of NSAIDs for inflammation management: Overview, progress, challenges and prospects. *International Journal of Pharmaceutics*, *515*(1–2), 757–773.

Baek, J.-S., & Cho, C.-W. (2015). Controlled release and reversal of multidrug resistance by co-encapsulation of paclitaxel and verapamil in solid lipid nanoparticles. *International Journal of Pharmaceutics*, *478*(2), 617–624.

Baek, J.-s., Yeo, E. W., Lee, Y. H., Tan, N. S., & Loo, S. C. J. (2017). Controlled-release nanoencapsulating microcapsules to combat inflammatory diseases. *Drug Design, Development and Therapy*, *11*, 1707–1717.

Berlin, R. G., Clineschmidt, B. V., & Majka, J. A. (1986). Famotidine: An appraisal of its mode of action and safety. *The American Journal of Medicine*, *81*(4), 8–12.

Bhattacharjee, S. (2016). DLS and zeta potential–what they are and what they are not? *Journal of Controlled Release*, *235*, 337–351.

Chang, Y., & McClements, D. J. (2014). Optimization of orange oil nanoemulsion formation by isothermal low-energy methods: Influence of the oil phase, surfactant, and temperature. *Journal of Agricultural and Food Chemistry*, *62*(10), 2306–2312. https://doi.org/10.1021/jf500160y.

Chang, Y., McLandsborough, L., & McClements, D. J. (2013). Physicochemical properties and antimicrobial efficacy of carvacrol nanoemulsions formed by spontaneous emulsification. *Journal of Agricultural and Food Chemistry*, *61*(37), 8906–8913. https://doi.org/10.1021/jf402147p.

Clarysse, S., Psachoulias, D., Brouwers, J., Tack, J., Annaert, P., Duchateau, G., Reppas, C., & Augustijns, P. (2009). Postprandial changes in solubilizing capacity of human intestinal fluids for BCS class II drugs. *Pharmaceutical Research*, *26*(6), 1456–1466.

Coradini, K., Friedrich, R. B., Fonseca, F. N., Vencato, M. S., Andrade, D. F., Oliveira, C. M., Battistel, A. P., Guterres, S. S., da Rocha, M. I. U. M., Pohlmann, A. R., & Beck, R. C. R. (2015). A novel approach to arthritis treatment based on resveratrol and curcumin co-encapsulated in lipid-core nanocapsules: in vivo studies. *European Journal of Pharmaceutical Sciences*, *78*, 163–170.

Costa, F., Sousa, J., Pais, A., & Formosinho, S. (2003). Comparison of dissolution profiles of ibuprofen pellets. *Journal of Controlled Release*, *89*(2), 199–212.

Costa, P., & Lobo, J. M. S. (2001). Modeling and comparison of dissolution profiles. *European Journal of Pharmaceutical Sciences*, *13*(2), 123–133.

de Souza, M. C., Vieira, A. J., Beserra, F. P., Pellizzon, C. H., Nóbrega, R. H., & Rozza, A. L. (2019). Gastroprotective effect of limonene in rats: Influence on oxidative stress, inflammation and gene expression. *Phytomedicine*, *53*, 37–42. https://doi.org/10.1016/j.phymed.2018.09.027.

Freeling, J. P., Koehn, J., Shu, C., Sun, J., & Ho, R. J. (2014). Long-acting three-drug combination anti-HIV nanoparticles enhance drug exposure in primate plasma and cells within lymph nodes and blood. *AIDS (London, England)*, *28*(17), 2625–2627.

Fritsche, E., Baek, S. J., King, L. M., Zeldin, D. C., Eling, T. E., & Bell, D. A. (2001). Functional characterization of cyclooxygenase-2 polymorphisms. *Journal of Pharmacology and Experimental Therapeutics*, *299*(2), 468–476.

Gadde, S. (2015). Multi-drug delivery nanocarriers for combination therapy. *Medicinal Chemistry Communications*, *6*(11), 1916–1929.

Giacomelli, C., Schmidt, V., & Borsali, R. (2007). Nanocontainers formed by self-assembly of poly(ethylene oxide)-b-poly(glycerol monomethacrylate)–drug conjugates. *Macromolecules*, *40*(6), 2148–2157. https://doi.org/10.1021/ma062562u.

Guarino, V., Gentile, G., Sorrentino, L., & Ambrosio, L. (2017). Polycaprolactone: Synthesis, properties, and applications. *Encyclopedia of Polymer Science and Technology*, 1–36.

Gursoy, R. N., & Benita, S. (2004). Self-emulsifying drug delivery systems (SEDDS) for improved oral delivery of lipophilic drugs. *Biomedicine & Pharmacotherapy*, *58*(3), 173–182.

Hassan, M. A., Salem, M. S., Sueliman, M. S., & Najib, N. M. (1997). Characterization of famotidine polymorphic forms. *International Journal of Pharmaceutics*, *149*(2), 227–232.

Higuchi, K., Umegaki, E., Watanabe, T., Yoda, Y., Morita, E., Murano, M., Tokioka, S., & Arakawa, T. (2009). Present status and strategy of NSAIDs-induced small bowel injury. *Journal of Gastroenterology*, *44*(9), 879–888.

Hochberg, M. C., Altman, R. D., April, K. T., Benkhalti, M., Guyatt, G., McGowan, J., Towheed, T., Welch, V., Wells, G., & Tugwell, P. (2012). American College of Rheumatology 2012 recommendations for the use of nonpharmacologic and pharmacologic therapies in osteoarthritis of the hand, hip, and knee. *Arthritis Care & Research*, *64*(4), 465–474.

Ignacio, M., Chubynsky, M. V., & Slater, G. W. (2017). Interpreting the Weibull fitting parameters for diffusion-controlled release data. *Physica A: Statistical Mechanics and its Applications*, *486*, 486–496.

Jaiswal, M., Dudhe, R., & Sharma, P. (2015). Nanoemulsion: An advanced mode of drug delivery system. *3 Biotech*, *5*(2), 123–127.

Koizumi, T., Ritthidej, G. C., & Phaechamud, T. (2001). Mechanistic modeling of drug release from chitosan coated tablets. *Journal of Controlled Release*, *70*(3), 277–284.

Koroleva, M., Nagovitsina, T., & Yurtov, E. (2018). Nanoemulsions stabilized by non-ionic surfactants: Stability and degradation mechanisms. *Physical Chemistry Chemical Physics*, *20*(15), 10369–10377. https://doi.org/10.1039/c7cp07626f.

Kosmidis, K., Argyrakis, P., & Macheras, P. (2003). A reappraisal of drug release laws using Monte Carlo simulations: The prevalence of the Weibull function. *Pharmaceutical Research*, *20*(7), 988–995.

Kuznetsova, D. A., Gabdrakhmanov, D. R., Kuznetsov, D. M., Lukashenko, S. S., Sapunova, A. S., Voloshina, A. D., Nizameev, I. R., Kadirov, M. K., & Zakharova, L. Y. (2020). Biocompatible supramolecular systems based on novel cationic imidazolium- and urethane-containing amphiphiles: Self-assembly and antimicrobial properties. *Journal of Molecular Liquids*, *319*, 114094. https://doi.org/10.1016/j.molliq.2020.114094.

Laroux, F. S. (2004). Mechanisms of inflammation: The good, the bad and the ugly. *Frontiers in Bioscience*, *9*, 3156–3162.

Li, P.-H., & Chiang, B.-H. (2012). Process optimization and stability of d-limonene-in-water nanoemulsions prepared by ultrasonic emulsification using response surface methodology. *Ultrasonics Sonochemistry*, *19*(1), 192–197. https://doi.org/10.1016/j.ultsonch.2011.05.017.

Lucas, S. (2016). The pharmacology of indomethacin. *Headache: The Journal of Head and Face Pain*, *56*(2), 436–446.

Mayer, B. X., Mensik, C., Krishnaswami, S., Derendorf, H., Eichler, H. G., Schmetterer, L., & Wolzt, M. (1999). Pharmacokinetic-pharmacodynamic profile of systemic nitric oxide-synthase inhibition with L-NMMA in humans. *British Journal of Clinical Pharmacology*, *47*(5), 539–544.

Mohsin, K., Long, M. A., & Pouton, C. W. (2009). Design of lipid-based formulations for oral administration of poorly water-soluble drugs: Precipitation of drug after dispersion of formulations in aqueous solution. *Journal of Pharmaceutical Sciences*, *98*(10), 3582–3595.

Moraes, T. M., Rozza, A. L., Kushima, H., Pellizzon, C. H., Rocha, L. R. M., & Hiruma-Lima, C. A. (2013). Healing actions of essential oils from Citrus aurantium and d-limonene in the gastric mucosa: The roles of VEGF, PCNA, and COX-2 in cell proliferation. *Journal of Medicinal Food*, *16*(12), 1162–1167. https://doi.org/10.1089/jmf.2012.0259.

Nair, L. S., & Laurencin, C. T. (2007). Biodegradable polymers as biomaterials. *Progress in Polymer Science*, *32*(8–9), 762–798.

Naito, Y., Iinuma, S., Yagi, N., Boku, Y., Imamoto, E., Takagi, T., Handa, O., Kokura, S., & Yoshikawa, T. (2008). Prevention of indomethacin-induced gastric mucosal injury in helicobacter pylori-negative healthy volunteers: A comparison study rebamipide vs famotidine. *Journal of Clinical Biochemistry and Nutrition*, *43*(1), 34–40.

Nathan, C. (2002). Points of control in inflammation. *Nature*, *420*(6917), 846–852.

Ong, C. K., Seymour, R. A., Lirk, P., & Merry, A. F. (2010). Combining paracetamol (acetaminophen) with nonsteroidal antiinflammatory drugs: A qualitative systematic review of analgesic efficacy for acute postoperative pain. *Anesthesia & Analgesia*, *110*(4), 1170–1179.

Perez-Aisa, A., Sopena, F., Arceiz, E., Ortego, J., Sainz, R., & Lanas, A. (2003). Effect of exogenous administration of transforming growth factor-beta and famotidine on the healing of duodenal ulcer under the impact of indomethacin. *Digestive and Liver Disease*, *35*(6), 397–403.

Ricciotti, E., & FitzGerald, G. A. (2011). Prostaglandins and inflammation. *Arteriosclerosis, Thrombosis, and Vascular Biology*, *31*(5), 986–1000.

Saeedi, M., Akbari, J., Morteza-Semnani, K., Enayati-Fard, R., Sar-Reshtehdar, S., & Soleymani, A. (2011). Enhancement of dissolution rate of indomethacin: Using liquisolid compacts. *Iranian journal of pharmaceutical research: IJPR*, *10*(1), 25–34.

Sostres, C., Gargallo, C. J., Arroyo, M. T., & Lanas, A. (2010). Adverse effects of non-steroidal anti-inflammatory drugs (NSAIDs, aspirin and coxibs) on upper gastrointestinal tract. *Best Practice & Research Clinical Gastroenterology*, *24*(2), 121–132.

Talke, P. O., & Solanki, D. R. (1993). Dose-response study of oral famotidine for reduction of gastric acidity and volume in outpatients and inpatients. *Anesthesia and Analgesia*, *77*(6), 1143-1148.

Tan, J., Deng, Z., Liu, G., Hu, J., & Liu, S. (2018). Anti-inflammatory polymersomes of redox-responsive polyprodrug amphiphiles with inflammation-triggered indomethacin release characteristics. *Biomaterials*, *178*, 608–619. https://doi.org/10.1016/j.biomaterials.2018.03.035.

Torchilin, V. P., & Trubetskoy, V. S. (1995). Which polymers can make nanoparticulate drug carriers long-circulating? *Advanced Drug Delivery Reviews*, *16*(2–3), 141–155.

Woodruff, M. A., & Hutmacher, D. W. (2010). The return of a forgotten polymer—Polycaprolactone in the 21st century. *Progress in Polymer Science*, *35*(10), 1217–1256.

Yeh, K. C. (1985). Pharmacokinetic overview of indomethacin and sustained-release indomethacin. *The American Journal of Medicine*, *79*(4), 3–12.

Zhang, Y., Huo, M., Zhou, J., Zou, A., Li, W., Yao, C., & Xie, S. (2010). DDSolver: An add-in program for modeling and comparison of drug dissolution profiles. *The AAPS Journal*, *12*(3), 263–271. http://dx.doi.org/10.1208/s12248-010-9185-1.

Ziltener, J.-L., Leal, S., & Fournier, P.-E. (2010). Non-steroidal anti-inflammatory drugs for athletes: An update. *Annals of Physical and Rehabilitation Medicine*, *53*(4), 278–288.

How to cite this article: Assali M, Zohud N. Design of multicomponent indomethacin-paracetamol and famotidine loaded nanoparticles for sustained and effective anti-inflammatory therapy. *Drug Dev Res*. 2020;1–10. https://doi.org/10.1002/ddr.21768